NASA TECHNICAL
MEMORANDUM

NASA TM X-52806

CASE FILE
COPY

ELECTROCHEMICAL BEHAVIOR OF THE BORON
ANODE IN AQUEOUS SOLUTIONS

by Betty S. Del Duca
Lewis Research Center
Cleveland, Ohio

ELECTROCHEMICAL BEHAVIOR OF THE BORON ANODE

IN AQUEOUS SOLUTIONS

by Betty S. Del Duca

Lewis Research Center
Cleveland, Ohio

ELECTROCHEMICAL BEHAVIOR OF THE BORON ANODE

IN AQUEOUS SOLUTIONS

by Betty S. Del Duca

NASA-Lewis Research Center
Cleveland, Ohio

ABSTRACT

The electrochemical oxidation of p-type boron in 0.2 N $NaNO_3$ solutions of pH 0.4-13.1 was studied by galvanostatic techniques. The capacitance of the electrode, Tafel slopes and a limited analysis of reaction mechanism is reported. The anodic dissolution in acid solution is a charge transfer limited one electron reaction to form a monovalent species in the over-potential region of .25 to .70 volts. The dissolution in basic solution is most probably a one electron charge transfer reaction from a mono-valent to divalent species involving three hydroxyl ions.

Open circuit potentials were mixed potentials, probably due to hydrogen formation at open circuit but not contributing to the electro-chemical reaction at the applied overpotential.

The level of illumination had no effect on the electrochemical behavior of the electrode.

E-5684

TM X-52806

ELECTROCHEMICAL BEHAVIOR OF THE BORON ANODE

IN AQUEOUS SOLUTIONS

by Betty S. Del Duca

NASA-Lewis Research Center
Cleveland, Ohio

SUMMARY

The electrochemical oxidation of p-type boron in 0.2 N $NaNO_3$ solutions of pH 0.4-13.1 at room temperature was studied by galvanostatic techniques.

The capacitance of the electrodes was found to be normal, 10.5 $\mu f/cm^2$ in acid solutions and 25.9 $\mu f/cm^2$ in basic electrolyte.

Tafel plots were constructed and the slopes used to determine the charge transfer rate determining reaction over the whole pH range. The reaction in acidic solution was found to be a one electron transfer $B \rightarrow B^+ + e^-$. The reaction $B^+ \rightarrow B^{++} + e^-$ was found to be most probable in basic solutions. Analysis of transition time data at low hydroxide concentrations suggest that three hydroxyl ions are involved in the rate determining step in basic solutions.

A value of 1.5 x 10^{-6} cm^2/sec was obtained for the diffusion coefficient of OH^- ion in 0.2 N $NaNO_3$.

Open circuit potentials did not agree with thermodynamically calculated values. The discrepancy was attributed to mixed potentials, probably due to hydrogen formation at the open circuit potential. Hydrogen formation did not contribute appreciably to the overall reaction at the applied overpotentials.

The level of illumination had no effect on the electrochemical behavior of the electrode.

INTRODUCTION

The high theoretical half-cell potential of boron makes it an interesting candidate for, as Fleischer (ref. 1) has pointed out, an anode in primary batteries. Boron is a lightweight, trivalent material second only to beryllium in both gravimetric and volumetric energy density. It is unreactive with most acids, alkalis and organic solvents (ref. 2). Possible oxide film formation, semiconductor behavior and high resistivity may be involved in its electrochemical performance.

The electrochemical properties of boron have received very little attention. Chen and Salomen (ref. 3) measured the anodic efficiency of boron anodes in 0.1 N LiOH solution at 30° C. Individual measurements varied from 84.0 to 121 percent current efficiency with an average of about 98 percent efficiency.

In this study, constant current steps were applied anodically to boron electrodes in a 0.2 NNaNO$_3$ solution varying in pH from 0.4-13.1. Measurement of the resultant potentials permitted the determination of the Tafel slope, the capacitance of the electrode and limited analysis of the mechanism of the reaction. The influence of the level of illumination on the electrochemical behavior was also investigated to determine if the boron electrode exhibits semiconductor properties.

EXPERIMENTAL

A. ELECTRODE

Boron filaments 4 mils (.01016 cm) in diameter deposited on a half mil (.00127 cm) core of tungsten were used as the electrode material in this study. Metallographs of a cross-section of the filament indicated

a homogeneous outer layer, presumably boron, with a second phase as a core. X-ray diffraction patterns obtained with both copper and chromium radiation showed the existence of WB_4 and W_2B_5 and no metallic tungsten in the core. No other compounds were present. Similar results are described by Warner and Satterfield (ref. 4) who have published metallographic cross-sections similar in appearance to those obtained in the present work. They also found evidence for a core composed solely of WB_4 and W_2B_5. They note that this composition results from vapor deposition of boron from a halide system.

Further evidence for the WB_4, W_2B_5-core was obtained by measuring the resistance of a given length of filament. The average resistivity was much larger than the value given by Touloukian (ref. 5) for tungsten $(5.2 \times 10^{-6} \ \Omega \ cm)$ and corresponded almost exactly to that given for a tungsten boride compound (not WB_4 or W_2B_5, however) of $55 \times 10^{-6} \ \Omega \ cm$.

Lipsitt (ref. 6) used electron diffraction techniques to study the nature of the filament surface and concluded the boron is a heavily faulted multi-layered crystalline structure which is stable at temperatures up to 1000° C over an extended period of time.

The thermoelectric probe technique (ref. 7) indicated that the filaments used in this work were p-type.

The filaments were mounted for electrochemical study to a copper conductor by heliarc techniques (tungsten inert gas welding in a nitrogen atmosphere). The bottom end was sealed with a transparent silicon rubber adhesive/sealant to prevent exposure of the core to the electrolyte.

All current densities are based upon the measured geometrical area of the electrode.

Metallographic studies of the filaments following electrolysis showed the removal of boron to be regular with no cracking or pitting at magnifications of up to 500 times.

B. ELECTROCHEMICAL CELL

The cell used is shown in figure 1. It consists of a Pyrex vessel containing a platinum cup which serves as the counter electrode. All potentials were measured relative to a commercial saturated calomel reference electrode with an asbestos thread junction encased in a glass envelope with a Luggin capillary. The working and reference electrodes were positioned in the center of the platinum cup. A Teflon magnetic stirrer was placed in the cell.

The electrolyte was 0.2 NNaNO$_3$ prepared from reagent grade NaNO$_3$ and distilled water and the pH was adjusted over the range from 0.5 to 13.1 as desired by the addition of reagent grade HCl or KOH. All experiments were done at room temperature.

C. INSTRUMENTATION

Constant current steps adjusted to provide current densities in the range from 0.3 to 10 ma/cm^2 were supplied to the electrode by means of a 1-3 μ sec. rise time potentiostat and a conventional relay-pulse generator shown schematically in figure 2. The resultant potential vs time curve was displayed on an oscilloscope with a differential amplifier having an input impedance of 1 megohm paralleled by 4.7 picofarads. Photographs were taken of the traces during the first 350 μ sec. following initiation of the pulse to permit calculation of the IR drop in the electrode and in

the solution between the electrode surface and the tip of the Luggin capillary by observation of the initial potential jump. In addition, the differential double layer capacitance was obtained from the slope of the initial linear potential rise $(\partial\eta/\partial t)_{t\to0}$ (figure 3(a)) from the equation:

$$C = \frac{i}{(\partial\eta/\partial t)_{t\to0}}$$

where i = applied current density

Photographs taken over the time interval of 0-140 msec permitted observation of the steady resultant potential. Figure 3(b) is typical of these photographs. In all cases, a steady potential was established within 80 msec.

The influence of illumination was investigated in the 0.5 NHCl electrolyte using a 500 watt incandescent photoflood 1 foot from the electrode room light and darkness. No differences in the electrochemical behavior were noted. Normal Tafel behavior and the absence of a photo-effect is expected for anodic dissolution reactions of p-type semiconductors by anology with germanium (ref. 8).

Open circuit potentials were measured relative to the saturated calomel reference with a high input impedance (> 5000 megohm) digital voltmeter. About a hour was required to reach a steady-state potential. Potentials were measured in the presence and absence of oxygen by bubbling either air or pure argon through the solution.

D. ANALYSIS OF DATA

Potentials, assumed to be activation overpotentials, read from the photographs at 120 msec. for various current density pulses were corrected

for the IR drop and plotted vs the log of the current density to give a Tafel plot. A straight line is indicative of a charge transfer rate determining step and the extrapolation of the straight line portion to the true $\eta = 0$ axis (equilibrium potential) gives the exchange current (i_0) for the reaction. The slope of the line ($\partial \log i/\partial\eta$) may be used to calculate an apparent anodic charge transfer coefficient (α), providing the charge-transfer valence, Z, is known: (ref. 9)

$$\alpha = \frac{(2.303)(\partial \log i/\partial\eta)RT}{ZF}$$

where
i = applied current density, ma/cm^2, + anodic, - cathodic

η = observed overpotential mV, + anodic, - cathodic

Z = charge transfer valence

F = Faraday

R = gas constant 8.314 vcoul/mole degree

T = temp. $^{\circ}K$

RESULTS AND DISCUSSION

A. ELECTRODE POTENTIALS

Table I lists open circuit potentials for 0.05, 0.25 and 0.40 M H_3BO_3 solutions with 0.20 N $NaNO_3$ and either 0.05 N HCl or 0.02 N KOH. All potentials are reported relative to the standard hydrogen electrode. Identical potentials were obtained in an Ar atmosphere and in air. The calculated values given in Table I are obtained from the Nernst relation and Latimer's (ref. 10) standard equilibrium potentials and ionization constants for (1) boron in acid solution: $3H_2O^+B \rightarrow H_3BO_3 + 3H^+ + 3e^-$, $E^0 = -0.87$ volts and (2) boron in basic solution: $B + 4O\ H^- \rightarrow H_2BO_3^- + H_2O + 3e^-$, $E^0 = 1.79$ volts. The experimental potentials

are much less anodic than the calculated values, indicating the possibility of reactions other than those assumed in the calculation of E^0 or a mixed potential due to additional reactions such as hydrogen formation. The second explanation appears most likely and will be discussed in detail below.

B. CAPACITANCE

The average differential capacitance of the electrode was 10.5 ± 1 $\mu farads/cm^2$ and 25.9 ± 2 $\mu farads/cm^2$ in acid and basic solution respectively. Capacitance values of this magnitude would indicate little if any oxide film formation in either pH range.

C. TAFEL BEHAVIOR

Straight lines were obtained in Tafel plots of all the data-indicating the existence of a charge-transfer rate determining process. Figure 4 for IN HCl electrolyte is typical, where the linear region extends from about 0.25 volts to about 0.70 volts. No limiting currents were observed. Tafel slopes are summarized in Table II for the electrolyte studies.

D. MIXED POTENTIALS

A mixed potential between B oxidation and H_2 reduction reactions would explain the near zero open circuit potential observed for acidic solutions; allow for pure charge transfer rate limited oxidation of boron in the anodic overpotential region of 0.25 - 0.70 volts; and explain the observed evolution of hydrogen with the application of cathodic currents.

If the open circuit potential is a mixed potential, dissolution of boron into the electrolyte should occur with time. Electrolytes in which boron anodes were allowed to stand for 300 hours contained undetectable amounts of
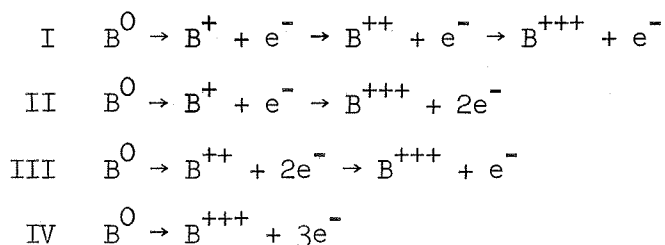
boron. Calculation shows, however, that corrosion currents as high as 0.7 ma/cm^2 would produce boron concentrations of 0.07 ppm in the 200 ml electrolyte volume - a concentration below the limit of detection of boron by chemical or atomic absorption techniques.

Experimental evidence has recently been acquired which indicates that the electrochemical cell is effectively loaded when the oscilloscope and galvanostate circuits are connected. This results in an electrode which is not at true open circuit potential prior to the application of the current step, and hence the potential at $\eta \to 0$ is not known at this time. This does not invalidate the Tafel slopes summarized in Table II but does prohibit the use of the open circuit potentials in Table II to place the polarization data at different pH values on the same potential scale. Thus, exchange currents and the determination of reaction order with respect to pH cannot be calculated from the data as presented. Further work is underway to correct this situation.

In acidic solutions, the Tafel slopes decrease with increasing pH, an effect which is not understood.

E. REACTION MECHANISM

The Fraser and Barrados' (ref. 11) method of quasi-equilibrium analysis of possible rate determining reactions was used to calculate Tafel slopes. The following consecutive anodic reactions were considered:

I $\quad B^0 \to B^+ + e^- \to B^{++} + e^- \to B^{+++} + e^-$

II $\quad B^0 \to B^+ + e^- \to B^{+++} + 2e^-$

III $\quad B^0 \to B^{++} + 2e^- \to B^{+++} + e^-$

IV $\quad B^0 \to B^{+++} + 3e^-$

The calculated Tafel slopes in terms of the true anodic transfer coefficient, β, appear in Table III. Comparison of these values with the measured slopes of Table II indicates that the most probable rate determining step for acid solutions is $B \rightarrow B^+ + e^-$ with $\beta \cong 0.22$. For basic solutions it is $B^+ \rightarrow B^{++} + e^-$ with $\beta \cong 0.56$. Three other reactions in basic solution give reasonable values of β between 0.2-1.0, but all involve two electrons and are therefore less probable due to the high activation energy required for multielectron transfers (ref. 12). They are:

$$B \rightarrow B^{++} + 2e^-$$
$$B \rightarrow B^{+++} + 3e^-$$
$$B^+ \rightarrow B^{+++} + 2e^-$$
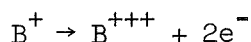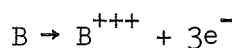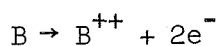
In addition to the Tafel results appearing in Table II data were also obtained using the slightly basic sodium nitrate electrolytes containing 0.001 N KOH and 0.002 N KOH. A transition time, τ, was observed in the potential traces obtained for these two electrolytes when current densities were less than 5 ma/cm^2. The inset of figure 5 is typical of such traces. The transition time is, of course, dependent upon the current density applied. This is not due to electrolytic removal of a surface layer since the total charge involved $q = i \tau$, is not constant. However, the product $i(\tau)^{1/2}$, summarized in Table V, is independent of current density with an average value of 0.31 and 0.63 for the 0.001 N and 0.002 N KOH solutions respectively. The constancy of the $i(\tau)^{1/2}$ product indicates a diffusion controlled electrode process (ref. 13). The observation of this effect only at low KOH concentrations, the proportionality of $i(\tau)^{1/2}$ to the KOH concentration and the consumption of OH$^-$ in the overall reaction suggests that

OH$^-$ is the diffusing species. Through the use of the Sand Equation (ref. 13, p. 237) a reasonable value of 1.5×10^{-6} cm^2/sec is obtained for the diffusion coefficient.

Again referring to the inset in fig. 5, the potential plateau prior to the transition time, τ, gives Tafel slopes similar to those obtained from the more basic 0.05 N KOH and 1 N KOH electrolytes. Table IV summarizes data from this plateau (time period 1) and data from the constant potential following τ (time period 2). The data from time period 2 also gives a linear Tafel plot (fig. 6) but must represent a mixed reaction including some diffusion of OH$^-$ to the surface. The Tafel slopes here are intermediate between the slopes for the acid and the basic electrolytes.

For the dilute KOH solutions, the overpotential-time behavior in time period 1 is characterized by a charge transfer limited reaction becoming partially diffusion controlled. Since the electrode is heavily polarized relative to the equilibrium potential, ($\eta \gg RT/nF$) the equation derived and discussed by Vetter (ref. 9, p. 357) can be used to advantage. A plot of the function log $(1 - \sqrt{t/\tau})$ vs η should be a straight line for the case where a species like OH$^-$ is being depleted by electrochemical reaction. Typical examples of these plots are shown in figure 5. The slope is equal to $(-1/b_a Z_{r,OH^-})$ where b_a is the Tafel slope (see Table IV) and Z_{r,OH^-} is the reaction order with respect to OH$^-$. A value of $Z_{r,OH^-} = 3.1$ is obtained. This implies that three OH$^-$ ions are involved in the rate determining charge transfer step. That is, for the one electron transfer

$$B^+ + 3OH^- \to B(OH)_3^- + 1e^-$$
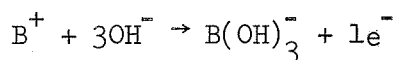
One cannot unambiguously rule out the possibility of a multi-electron rate determining step on the basis of the Tafel data and hence reactions:

$$B + 3OH^- \rightarrow B(OH)_3^- + 2e^-,$$

$$B + 3OH^- \rightarrow B(OH)_3 + 3e^-, \text{ or}$$

$$B^+ + 3OH^- \rightarrow B(OH_3) + 2e^-$$
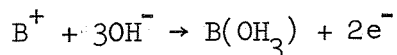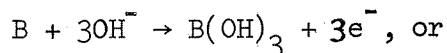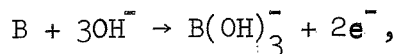
could also be invoked in basic solution though they are less likely for reasons already mentioned.

Transition times were not observed for 0.05 N KOH and 1 N KOH solutions. In these cases, the concentrations of OH^- is so great that large current densities and long electrolysis times would be required to deplete the OH^- near the electrode. The largest current density used, 4.5 ma/cm^2 would have a transition time of 40 seconds in 0.05 N KOH electrolyte. The current step actually lasted only about 0.2 seconds.
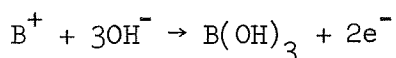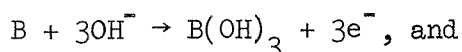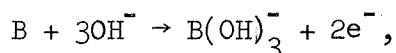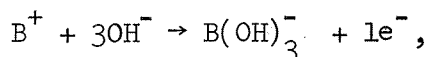
CONCLUSIONS

P-type boron appears to undergo uniform dissolution in 0.2 N sodium nitrate electrolytes over a range of pH from 0.4 to 13.1 without pitting or cracking. The major component of the resistance of the electrode appears to be due to the tungsten boride core, so that the conductance could conceivably be improved by the deposition of boron upon a more suitable electronic conductor. No variation in the current-voltage behavior with illumination was noted.

Neither acid nor basic electrolyte systems achieved the thermodynamic equilibrium potential, a situation attributed to a mixed potential arising from the hydrogen evolution reaction. This complication precluded the determination of exchange currents without further measurements.

The capacitance of the electrode is normal. Values of 10.5 $\mu f/cm^2$ and 25.9 $\mu f/cm^2$ were obtained for acidic and basic solutions respectively.

In the anodic overpotential region of 0.25-0.75 volts, the reaction appears to be charge-transfer limited in both acidic and basic solutions. The rate determining step in acidic solutions from consideration of Tafel slopes appears to be the one electron transfer $B \rightarrow B^+ + 1e^-$. The rate determining step in basic solution is somewhat ambiguous. Consideration of Tafel slopes and the reaction order with respect to OH^-, determined chronopotentiometrically, leads to four possible rate determining reactions:

$$B^+ + 3OH^- \rightarrow B(OH)_3^- + 1e^-,$$
$$B + 3OH^- \rightarrow B(OH)_3^- + 2e^-,$$
$$B + 3OH^- \rightarrow B(OH)_3 + 3e^-, \text{ and}$$
$$B^+ + 3OH^- \rightarrow B(OH)_3 + 2e^-$$

The one electron transfer is most probable on energetic grounds.

The diffusion coefficient for OH^- in 0.2 N $NaNO_3$ solution was estimated to be 1.5 x 10^{-6} cm^2/sec from transition time determinations.

REFERENCES

1. A. Fleischer, "Survey and Analysis on Metal-Air Cells," Chemical and Metallurgical Research Inc., AFAPL-TR-68-6, AD-829289 (1968).

2. T. Moeller, "Inorganic Chemistry," John Wiley & Sons, New York (1952), p. 746.

3. L. C. Chen and R. E. Salomon, J. Electrochem. Soc., 110, 173 (1963).

4. F. E. Warner and D. B. Satterfield, Appl. Phys. Letters, 11, 192 (1967).

5. Y. S. Touloukian, "Thermophysical Properties of High Temperature and Solid Materials," Vol. 6, Part II, Macmillan Co., New York (1967).

6. H. A. Lipsitt, "Proceedings of the OAR Research Applications Conference,"
   Office of Aerospace Research, AD-631727 (1966), p. 141.

7. I. B. Gadoff and E. Miller, "Thermoelectric Materials and Devices,"
   Reinhold Publ. Co., New York (1960), p. 84.

8. W. H. Brittain and C. G. B. Garrett, Bell Syst. Tech. J., 34, 129 (1955).

9. K. J. Vetter, "Electrochemical Kinetics," Academic Press, New York (1967),
   p. 143.

10. W. M. Latimer, "Oxidation Potentials," Prentice-Hall, Englewood Cliffs,
    N. J. (1952), p. 279.

11. G. H. Fraser and R. G. Barrados, J. Electrochem. Soc., 112, 462 (1965).

12. J. O'M. Bockris and G. A. Razumney, "Fundamental Aspects of Electro-
    crystallization," Plenum Press, New York (1967), p. 36.

13. B. E. Conway, "Theory and Principles of Electrode Processes," Ronald
    Press, New York (1965), p. 118.

Table I

OPEN CIRCUIT POTENTIALS-BORON (VS SHE)

IN 0.20 M$NaNO_3$

A. Acid Solution - 0.05 N HCl		
Conc. of H_3BO_3 moles/l	Observed, V	Calculated
0.05	+.008±.011	-1.08
0.25	-.001±.033	-1.06
0.40	+.028±.006	-1.06

B. Basic Solution - 0.02 N KOH		
Conc. of H_3BO_3 moles/l	Observed, V	Calculated
0.05	+.344	-1.68
0.25	+.281	-1.67
0.40	+.198	-1.66

Table II

TAFEL SLOPES, OPEN CIRCUIT POTENTIALS - BORON

ANODES IN ACIDIC AND BASIC SOLUTIONS

Electrolyte	pH	Tafel Slope b_a	Open-Circuit Potential, vs She, Volts
0.2 N $NaNO_3$+ IN HCl	0.4	2.303 RT/.052±.003)(3F)	-.009±.019
0.2 N $NaNO_3$+ .05 N HCl	1.70	2.303 RT/(0.68±.003)(3F)	+.132±.006
0.2 N $NaNO_3$+ .002 N HCl	2.70	2.303 RT/(.087±.003)(3F)	+.158±.046
0.2 N $NaNO_3$	5.45	2.303 RT/(.084±.005)(3F)	+.228±.005
0.2 N $NaNO_3$+ .05 N KOH	11.9	2.303 RT/(.603±.03)(3F)	+.594±.012
0.2 N $NaNO_3$+ IN KOH	13.1	2.303 RT/(.435±.03)(3F)	+.671±.008

Table III

CALCULATED TAFEL SLOPES

Mech.	R.D.S.	b_a, Anodic Tafel Slope
I,II	$B^+ \rightarrow B^+ + e^-$	$2.303\ RT/\beta F$
I	$B^+ \rightarrow B^{++} + e^-$	$2.303\ RT/(\beta+1)F$
I,III	$B^{++} \rightarrow B^{+++} + e^-$	$2.303\ RT/(\beta+2)F$
III	$B^0 \rightarrow B^{++} + 2e^-$	$2.303\ RT/(2\beta)F$
IV	$B^0 \rightarrow B^{+++} + 3e^-$	$2.303\ RT/(3\beta)F$
IV	$B^+ \rightarrow B^{+++} + 2e^-$	$2.303\ RT/(2\beta+1)F$

Table IV

TAFEL SLOPES - BORON ANODES IN

.001 N KOH AND .002 N KOH ELECTROLYTE

Electrolyte	pH	Time Period	Tafel Slope
.2 N NaNO$_3$+ .001 N KOH	10.3	(1)	2.303 RT/(0.576±.06)(3)(F)
		(2)	2.303 RT/(0.255±.03)(3)(F)
.2 N NaNO$_3$+ .002 N KOH	10.7	(1)	2.303 RT/(0.540±.05)(3)(F)
		(2)	2.303 RT/(0.291±.04)(3)(F)

Table V

$i\sqrt{\tau}$ AT VARIOUS CURRENT DENSITIES

a) .002 N KOH	
i, ma/cm^2	$i\sqrt{\tau}$, $\dfrac{\text{ma(sec)}^{1/2}}{\text{cm}^2}$
.790	.70
1.13	.77
1.39	.67
2.10	.51
2.40	.63
2.73	.60
	av 0.63±.05

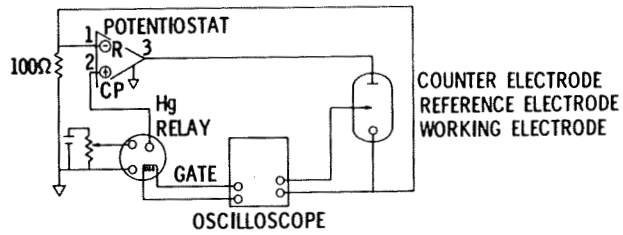| b) .001 N KOH	
i, ma/cm^2	$i\sqrt{\tau}$, $\dfrac{\text{ma(sec)}^{1/2}}{\text{cm}^2}$
.50	.33
.645	.32
.790	.19
.905	.31
1.13	.38
	av 0.31±.05

ELECTROCHEMICAL CELL
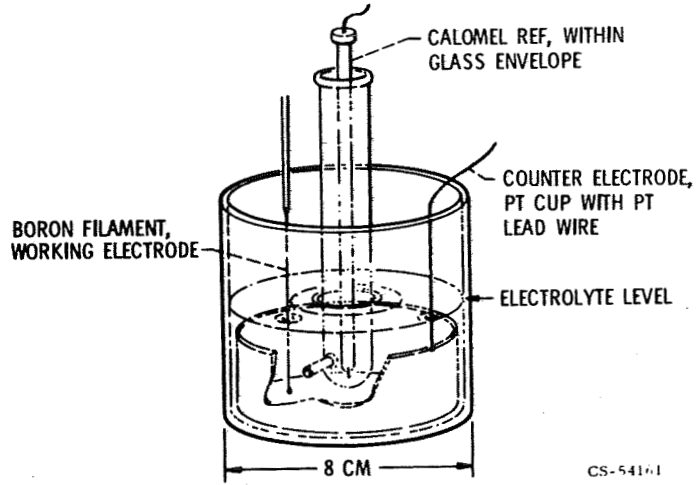
Figure 1
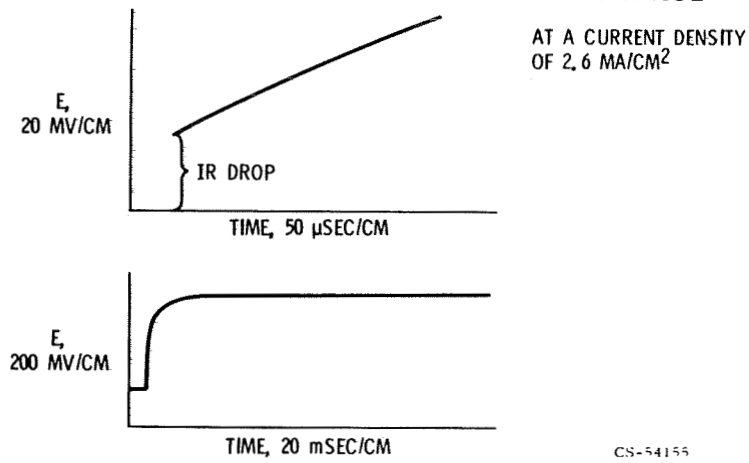
BLOCK DIAGRAM OF CIRCUIT
FOR GALVANOSTATIC MEASUREMENTS

1 REFERENCE ELECTRODE
2 CONTROL POTENTIAL
3 COUNTER ELECTRODE

Figure 2
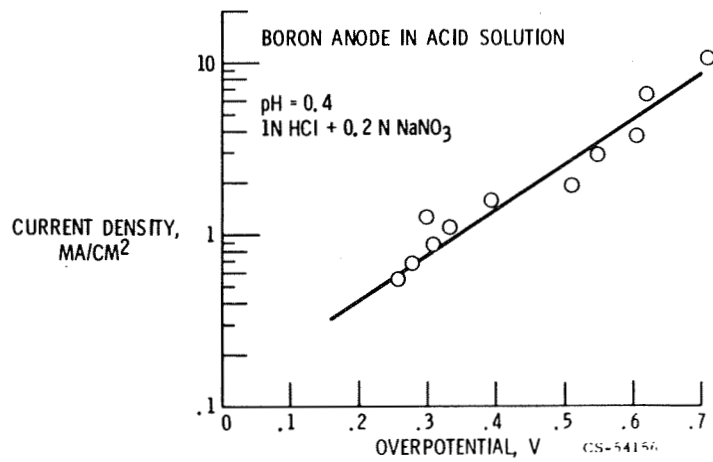
SHORT AND LONG TIME PHOTOGRAPHS
OF POTENTIAL—TIME CURVES FOR BORON ANODE

AT A CURRENT DENSITY
OF 2.6 MA/CM^2

E,
20 MV/CM

} IR DROP

TIME, 50 μSEC/CM

E,
200 MV/CM

TIME, 20 mSEC/CM

CS-54155

Figure 3

TAFEL PLOT

BORON ANODE IN ACID SOLUTION

pH = 0.4
1N HCl + 0.2 N NaNO$_3$

10

CURRENT DENSITY,
MA/CM^2

1

.1

0   .1   .2   .3   .4   .5   .6   .7
OVERPOTENTIAL, V   CS-54156
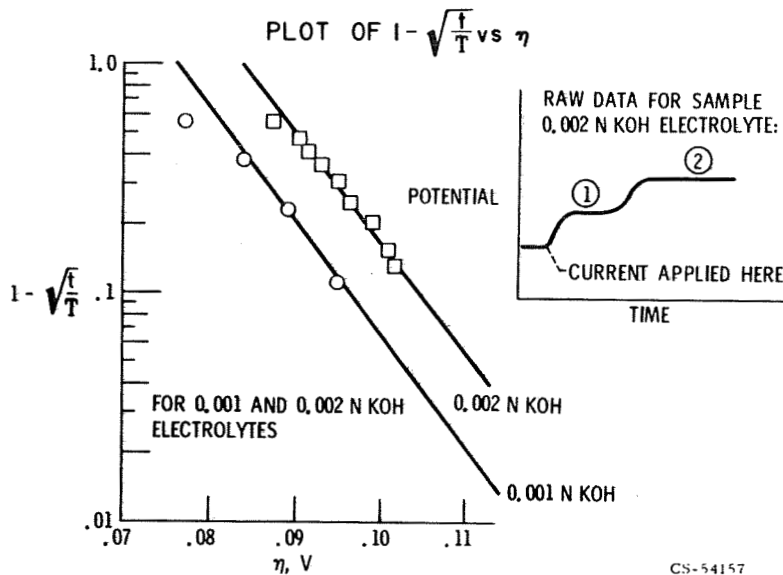
Figure 4

PLOT OF $1-\sqrt{\frac{t}{T}}$ vs η

Figure 5

CORRESPONDENCE OF TAFEL SLOPES FOR .05 N KOH AND 1 NKOH
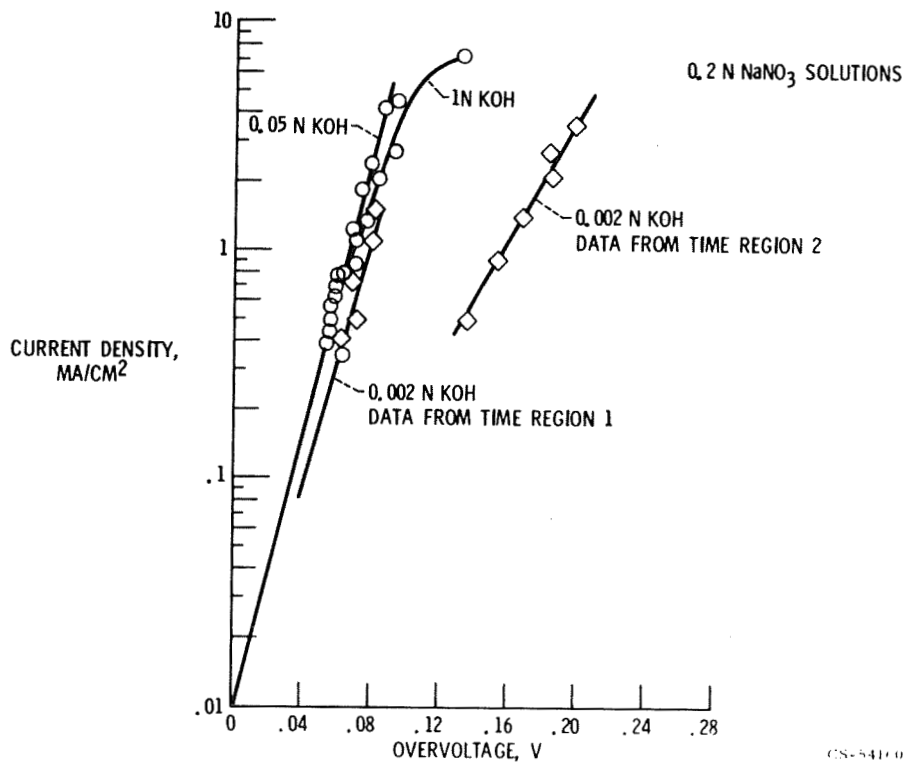ELECTROLYTE AND TIME REGION ① OF .002 N KOH ELECTROLYTE

Figure 6

CS-54157

CS-541₤0

NASA-Lewis-Com'l